Journal of Advanced Research 25 (2020) 125–136

Contents lists available at ScienceDirect

Journal of Advanced Research

journal homepage: www.elsevier.com/locate/jare

Research Article

Increasing the damping of oscillatory systems with an arbitrary number of time varying frequencies using fractional-order collocated feedback

V. Feliu-Batlle [a,*], D. Feliu-Talegon [b], A. San-Millan [c]

[a] Escuela Tecnica Superior de Ingenieros Industriales, Universidad de Castilla-La Mancha, Ciudad Real 13071, Spain
[b] Robotics, Vision and Control Group, University of Seville, 41092 Seville, Spain
[c] Instituto de Investigaciones Energeticas y Aplicaciones Industriales (INEI), Campus Universitario de Ciudad Real, 13071 Ciudad Real, Spain

GRAPHICAL ABSTRACT

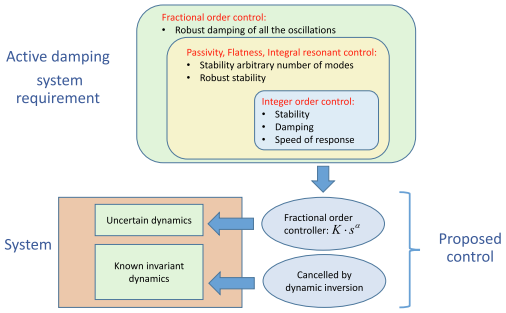

ARTICLE INFO

Article history:
Received 29 March 2020
Revised 22 May 2020
Accepted 9 June 2020
Available online 20 June 2020

Keywords:
Fractional-order controllers
Active vibration damping
Frequency domain control techniques
Robustness to large variations of vibration frequencies
Isophase margin systems

ABSTRACT

This paper studies the active damping of the oscillations of lightly damped linear systems whose parameters are indeterminate or may change through time. Systems with an arbitrary number of vibration modes are considered. Systems described by partial differential equations, that yield an infinite number of vibration modes, can also be included. In the case of collocated feedback, i.e. the sensor is placed at the same location of the actuator, a simple fractional order differentiation or integration of the measured signal is proposed that provides an effective control: (1) it guarantees a minimum phase margin or damping of the closed-loop system at all vibration modes, (2) this feature is robustly achieved, i.e., it is attained for very large variations or uncertainties of the oscillation frequencies of the system and (3) it is robust to spillover effects, i.e., to the unstabilizing effects of the vibration modes neglected in the controller design (especially important in infinite dimensional systems). Moreover, the sensitivity of the gain crossover frequency to such variations is assessed. Finally, these results are applied to the position control of a single link flexible robot. Simulated results are provided.

Introduction

Linear undamped systems appear in many scientific and technological areas, and their oscillations often have undesirable effects. Then, these oscillations have to be damped either by passive or active methods. In the first case, the system is redesigned by adding elements that physically damp the oscillations. In the second case, a feedback control law is closed around the undamped system in such a way that the oscillations of the whole system are reduced. These methods are tailored to the oscillation frequencies of the system, which are assumed to be time invariant.

☆ Peer review under responsibility of Cairo University.
* Corresponding author.
E-mail address: Vicente.Feliu@uclm.es (V. Feliu-Batlle).

https://doi.org/10.1016/j.jare.2020.06.008
2090-1232/

However, there are many applications in which the frequencies of the oscillations are time varying (*TVF* oscillations). In these cases, both passive and active dampers become untuned and their performances are significantly degraded. The need of damping *TVF* oscillations appears in many fields. Some examples are given next. In electrical engineering, *TVF* oscillations appear in the flexible AC transmission systems used to damp power system oscillations whose frequencies vary as consequence of changes in the operating target setpoint of the nonlinear power network or changes in the characteristics of some generators [1]. In power electronics, oscillations have to be damped in voltage compensation using dynamic voltage restorers (DVR), in which the *ac* source may experience variations of ± 2 Hz [2]. Combustion driven oscillations may appear in industrial combustors, where their frequencies vary according to the temperature and velocity distribution of the involved fluids [3]. Controllers of mechanical systems have to deal with *TVF* oscillations in tasks such as the sway reduction of bridge and granty cranes in which the frequencies change with the length of the suspension cable [4]. *TVF* oscillations whose frequencies change largely can only be damped by active systems.

Frequency methods are often used to design control laws for the active damping of oscillations in linear time invariant (*LTI*) systems. Phase and gain margins are measures of the relative stability of a system. Moreover, some temporal features of the closed-loop system are related to features of the open-loop frequency response. In particular, phase margin ϕ is related to damping and gain crossover frequency ω_c to system bandwidth and, hence, to speed of response ([5]).

Robust controllers based on the frequency domain methods have been designed to tackle the problem of damping *TVF* oscillations. Some mechanical examples are given next. Robust controllers were developed for structural vibration suppression using H_∞ methods in [6], for a compact disc player using the μ-framework in [7] and for flexible manipulators using the *QFT* method in [8].

Another approach to the robust damping of oscillations is to attain a frequency response that has a flat phase around the nominal gain crossover frequency. This feature achieves a constant phase margin when some plant parameters change. This is called the *isophase margin property* and implies that the closed-loop system damping and overshoot also remain approximately constant. Fractional-order control laws that attain this *local* isophase margin property (a survey is [9]) have been used to actively damp *TVF* oscillations. For example, Ref. [10] proposed a fractional-order proportional-derivative controller for the attitude control of a flexible spacecraft and [11] a fractional-order derivative controller for vehicle suspensions.

Nonlinear control techniques have been used to damp *TVF* oscillations too, like adaptive control in [12], neural network controllers in [13], or sliding controllers in [14]. Adaptive control has the drawbacks of: (a) the difficulty of guaranteeing closed loop stability, which usually requires a complicated Lyapunov stability analysis; (b) needing a persistent excitation in order to achieve an accurate estimation of the system parameters; (c) the worsen of the transient response during the term from the beginning of the transient until the plant parameters are estimated and the controller is retuned, which leads to tracking errors that may be unacceptable. Drawbacks of neural network control are that it is also difficult to guarantee the stability of the control system and it requires a previous - often laborious - network training process. Application of sliding control needs the fulfilment of the so called matching condition, which means that the uncertainties must remain in the space range of the control input to ensure an invariance property of the system behavior during the sliding mode, which sometimes may be troublesome. Moreover, the performance of the system is not well controlled during the term of reaching the sliding surface.

The previous controls damp *TVF* oscillations with small frequency variations, but they fail and even unstabilize the system if the oscillation frequencies experience very large variations or have very large uncertainties (of more than a decade above or below their nominal values). Moreover, these controllers are well suited only for systems having a finite (usually low) number of oscillations. They could be applied to systems having an infinite number of vibrations - like flexible mechanical structures - only if their infinite dimensional models were truncated yielding reduced order models with a finite number of oscillations. Such oscillations are damped by these controllers, but the neglected oscillations could unstabilize the closed-loop system. This is called the *spillover effect*, it can be hardly avoided using the above mentioned control techniques, and it is nearly impossible to deal with if the oscillation frequencies vary largely.

Systems with an infinite number of oscillations can be damped using control techniques based on the pole-zero interlazing (*PZI*) property. *PZI* property is achieved if the actuator and sensor of the closed-loop system are placed exactly at the same position. This configuration is denoted *collocated feedback* and yields controllers insensitive to spillover effects. Using this property, passivity (e.g. [15]), flatness (e.g. [16]) based feedback laws have been developed, as well as the integral resonant control (a recent nonlinear version of this is [17]). These techniques guarantee robust stability but do not achieve phase margin robustness, i.e, approximate damping robustness of all the vibration modes.

Some results have recently been obtained using fractional order controllers combined with the *PZI* property that improve the active damping robustness of systems with an arbitrary number of oscillation modes. In [18] the integrator of the integral resonant control was substituted by a fractional-order integrator. This improved the robustness of the damping of the lowest four vibration modes in the sense that the phase margins associated to these four modes were increased and the changes of these phase margins produced by changes of up to $\pm 40\%$ of the oscillation frequencies were lower than if the integral resonant control were used. In [19] a fractional-order controller combined with a passivity property was designed in order to obtain the local isophase margin property in the first vibration mode of flexible link robots. This outperformed significantly the damping robustness achieved with the previous controller to frequency changes in that mode. These two control systems have spillover robustness, i.e, the infinite modes neglected in the controller design remained stable, but the damping of these modes could not be designed. Finally, a very simple fractional-order controller was proposed in [20] for undamped systems that is robust to spillover and guarantees a constant phase margin of an arbitrary number of vibration modes, i.e, the same damping could be designed for all the modes, when the frequencies and gains of all the vibration modes change arbitrarily.

In this article, the results of [20] for undamped systems are extended to damped systems. Moreover, the robustness of the gain crossover frequency is assessed.

The paper is organized as follows. Section 2 recalls the results of [20] used here. Section 3 studies the gain crossover frequency robustness of the proposed controllers in the case of undamped systems. Section 4 obtains phase margin and gain crossover frequency robustness conditions for damped systems. Section 5 applies these results to control a single link flexible robot and some conclusions are exposed in Section 6.

Preliminary results

Consider a single-input single-output linear plant whose transfer function can be split into two factors:

$$G(s,\mathbf{p}) = \widehat{G}(s)P(s,\mathbf{p}). \tag{1}$$

The factor $\widehat{G}(s)$ is a rational transfer function that contains the known part of the plant, which is assumed to be stable and minimum phase. The factor $P(s,\mathbf{p})$ is a rational transfer function that contains the uncertain part of the plant, in which vector $\mathbf{p} \in \mathscr{P}$ represents the set of uncertain parameters, being $\mathscr{P}$ the region of admissible parametric vectors.

Assume that $P(s,\mathbf{p})$ is an oscillatory system with n undamped vibration modes:

$$P(s,\mathbf{p}) = \frac{b}{s^2+a_1^2}\prod_{i=1}^{n-1}\left(\frac{s^2+z_i^2}{s^2+a_{i+1}^2}\right) \tag{2}$$

whose parameters are grouped as $\mathbf{p} = (b, a_1, a_2, \ldots, a_n, z_1, z_2, \ldots, z_{n-1})$ being sorted in order of increasing values: $a_i < a_{i+1}$ and $z_i < z_{i+1}, \forall i$. Assume that all these parameters are positive, which is expressed as $\mathbf{p} > 0$. The nominal transfer function $P(s,\mathbf{p}_0)$ is defined by the nominal parameters b_0, $a_{i,0}$ and $z_{i,0}, \forall i$.

The magnitude of the frequency response of $P(s,\mathbf{p})$ is represented by

$$\Upsilon(x,\mathbf{p}) = |P(jx\omega_{c0},\mathbf{p})| \tag{3}$$

where $x = \omega/\omega_{c0}$ is the normalized frequency with respect to ω_{c0}, ω_{c0} being the gain crossover frequency desired for the controlled system in the case of the nominal parameters $\mathbf{p}_0$.

The *pole-zero interlacing property on the imaginary axis* is defined as the pattern that some transfer functions of undamped or lowly damped systems have of alternating the values of the imaginary components of their poles and zeros. This pole-zero pattern will hereafter be denoted by the *PZI* property. Assume that $P(s,\mathbf{p})$ has the *PZI* property, i.e, transfer function (2) verifies that $a_i < z_i < a_{i+1}, 1 \leqslant i < n-1$.

Fig. 1 shows the frequency response of a system (2) that verifies the *PZI* property (the case of $n = 3$ is represented).

The following results are recalled from [20] and are the starting point of this article. The feedback control structure used in this article is shown in Fig. 2.

Lemma 1. A transfer function $P(s,\mathbf{p})$ of the form (2) verifying the *PZI* property can always be expanded as

$$P(s,\mathbf{p}) = \sum_{i=1}^{n}\frac{k_i}{s^2+a_i^2}, k_i > 0, 1 \leqslant i \leqslant n, \tag{4}$$

and any transfer function that can be expanded in the form (4) verifies the *PZI* property.

Theorem 1. Consider a plant $G(s,\mathbf{p})$ of the form (1), (2) where $P(s,\mathbf{p})$ verifies the *PZI* property for any $\mathbf{p} > 0, \mathbf{p} \in \mathscr{P}$, representing $\mathscr{P}$ the set of all possible plants. The simplest controller $C(s)$, which:

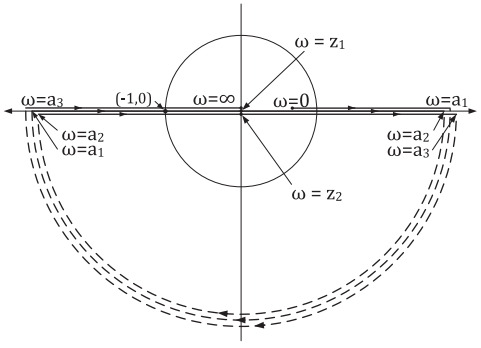

Fig. 1. Nyquist plot of P(s,**p**) verifying the *PZI* property.

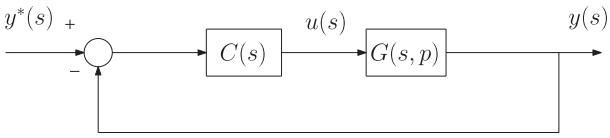

Fig. 2. Feedback control system.

1. maintains a desired phase margin ϕ_0 $(0 < \phi_0 \leqslant \pi/2$ rads) of $G(s,\mathbf{p})C(s)$ in the entire range of variation of $\mathbf{p}$,
2. yields a desired gain crossover frequency value ω_{c0} defined in the range $a_{1,0} < \omega_{c0} < z_{1,0}$ for the nominal set of parameters $\mathbf{p}_0$,

consists of the series connection of a fractional-order differentiator controller (hereafter denoted as the *FD* controller) and the inverse of the well determined part of the dynamics of the plant:

$$C(s) = \underbrace{\frac{1}{\Upsilon(1,\mathbf{p}_0)\omega_{c0}^{\alpha}}s^{\alpha}}_{FD\ controller}\widehat{G}^{-1}(s) \tag{5}$$

where α is a positive value:

$$\alpha = \frac{2}{\pi}\phi_0 \tag{6}$$

Moreover, the function $\omega_c = f(\mathbf{p})$ that describes the relationship yielded by this controller between the gain crossover frequency ω_c and the varying parameters is implicitly given by

$$x^{\alpha}\Upsilon(x,\mathbf{p}) = \Upsilon(1,\mathbf{p}_0);\ \ x = \frac{\omega_c}{\omega_{c0}} \tag{7}$$

where Υ is defined by (3). In the interval $\left(\frac{a_1}{\omega_{c0}}, \frac{z_1}{\omega_{c0}}\right)$, Eq. (7) has only one real positive solution x for any value $\mathbf{p} \in \mathscr{P}$, which verifies that

$$max\left(\frac{a_1}{\omega_{c0}}, x^*\right) < x < \frac{z_1}{\omega_{c0}} \tag{8}$$

being x^* the solution of the equation $\Upsilon(1,\mathbf{p}_0)x^{2-\alpha} = \Upsilon(x,\mathbf{p})\left(x^2 - \frac{a_1^2}{\omega_{c0}^2}\right)$

Fig. 3a shows the Nyquist plot of $L(j\omega,\mathbf{p}) = G(j\omega,\mathbf{p})C(j\omega)$. It illustrates that ϕ_0 can not be higher than 90° because, in that case, the Nyquist plot at interval $0 \leqslant \omega < a_1$ would cross the unit circle in the second quadrant, at a point closer to the negative real semi-axis than the point at which the Nyquist plot at interval $a_1 \leqslant \omega < z_1$ crosses the unit circle. This invalidates the ϕ_0 phase margin specification.

Theorem 2. Consider a plant $G(s,\mathbf{p})$ of the form (1), (2) where $P(s,\mathbf{p})$ verifies the *PZI* property for any $\mathbf{p} > 0, \mathbf{p} \in \mathscr{P}$, representing $\mathscr{P}$ the set of all possible plants. The simplest controller $C(s)$, which:

1. maintains a desired phase margin $-\phi_0$ $(0 < \phi_0 \leqslant \pi/2$ rads) of $G(s,\mathbf{p})C(s)$ in the entire range of variation of $\mathbf{p}$,
2. yields a desired gain crossover frequency value ω_{c0} defined in the range $\omega_{c0} < a_{1,0}$, for the nominal set of parameters $\mathbf{p}_0$,

consists of the series connection of a *FD* controller and the inverse of the well determined part of the dynamics of the plant given by expression (5), in which α is a positive value:

$$\alpha = 2 - \frac{2}{\pi}\phi_0 \tag{9}$$

Moreover, the function $\omega_c = f(\mathbf{p})$ that describes the relationship yielded by this controller between the gain crossover frequency and the varying parameters is implicitly given by (7). In the interval $\left(0, \frac{a_1}{\omega_{c0}}\right)$, Eq. (7) has only one real positive solution for any value $\mathbf{p} \in \mathscr{P}$.

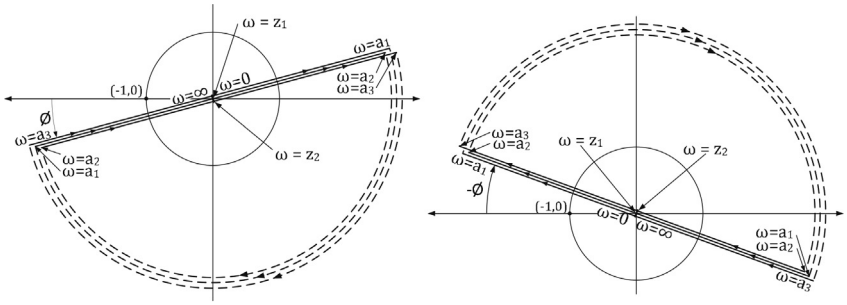

Fig. 3. Nyquist diagrams of the open-loop responses with controllers of: (a) Theorem 1 and (b) Theorem 2.

Fig. 3b shows the Nyquist plot of $L(j\omega,\mathbf{p}) = G(j\omega,\mathbf{p})C(j\omega)$. It illustrates that ϕ_0 can not be higher than 90° because, in that case, the Nyquist plot at interval $a_1 \leqslant \omega < z_1$ would cross the unit circle in the third quadrant, at a point closer to the negative real semiaxis than the point at which the Nyquist plot at interval $0 \leqslant \omega < a_1$ crosses the unit circle. This invalidates the $-\phi_0$ phase margin specification.

The $f(\mathbf{p})$ function

The previous theorems are useful to design controllers that guarantee an invariant phase margin in the case of large changes of parameters (either gains or vibration frequencies) of up to infinite-dimensional oscillatory systems (n in (2) is an arbitrary number that could be ∞). But no attention was paid to the gain crossover frequency robustness attained with these controllers. This is the objective of this section. The starting point is expression (7). Achieving robustness on the gain crossover frequency means that large variations in $\mathbf{p}$ involve small variations in the ω_c yielded by the function $\omega_c = f(\mathbf{p})$. The following two theorems develop some results about this issue.

Theorem 3. Consider a plant $G(s,\mathbf{p})$ of the form (1), (2) where $P(s,\mathbf{p})$ verifies the *PZI* property, and $\mathbf{p} \in \mathscr{P}$ such that $\mathbf{p} > 0$ and $\mathscr{P}$ represents the set of all possible plants. Assume a controller $C(s)$ given by expressions (5) and (6) of Theorem 1. The sensitivity of the gain crossover frequency ω_c to changes in the plant parameters has the following properties:

1. Function $f(\mathbf{p})$ is an increasing function in the parameters $p_k, 1 \leqslant k \leqslant 2$, (b, a_1) and $n+2 \leqslant k \leqslant 2n$, (z_i) and is decreasing in the parameters $p_k, 3 \leqslant k \leqslant n+1$, $(a_2 \ldots a_n)$.
2. The sensitivity of the gain crossover frequency ω_c, i.e., the variation of ω_c around ω_{c0} when parameters $\mathbf{p}$ vary around $\mathbf{p}_0$, increases if the design phase margin ϕ_0 increases.

Proof. According to (8), ω_c belongs to the interval $a_1 < \omega_c < z_1$, i.e, its normalized value x belongs to $\left(\frac{a_1}{\omega_{c0}}, \frac{z_1}{\omega_{c0}}\right)$. Since function

$$\Upsilon(x,\mathbf{p}) = \frac{\frac{b}{\omega_{c0}^2}}{x^2 - \left(\frac{a_1}{\omega_{c0}}\right)^2} \prod_{i=1}^{n-1} \left(\frac{\left(\frac{z_i}{\omega_{c0}}\right)^2 - x^2}{\left(\frac{a_{i+1}}{\omega_{c0}}\right)^2 - x^2} \right) \tag{10}$$

is positive in that interval, it is obtained that

$$\ln(\Upsilon(x,\mathbf{p})) = \ln\left(\frac{b}{\omega_{c0}^2}\right) - \ln\left(x^2 - \left(\frac{a_1}{\omega_{c0}}\right)^2\right) + \sum_{i=1}^{n-1} \left(\ln\left(\left(\frac{z_i}{\omega_{c0}}\right)^2 - x^2\right) - \ln\left(\left(\frac{a_{i+1}}{\omega_{c0}}\right)^2 - x^2\right) \right) \tag{11}$$

Differentiating this expression with respect to x and denoting $\partial\Upsilon/\partial x$ as Υ_x yields that

$$\frac{\Upsilon_x(x,\mathbf{p})}{2x\Upsilon(x,\mathbf{p})} = -\frac{1}{x^2 - \left(\frac{a_1}{\omega_{c0}}\right)^2} - \sum_{i=1}^{n-1} \frac{\left(\frac{a_{i+1}}{\omega_{c0}}\right)^2 - \left(\frac{z_i}{\omega_{c0}}\right)^2}{\left(\left(\frac{z_i}{\omega_{c0}}\right)^2 - x^2\right)\left(\left(\frac{a_{i+1}}{\omega_{c0}}\right)^2 - x^2\right)} \tag{12}$$

which is negative in the interval $x \in \left(\frac{a_1}{\omega_{c0}}, \frac{z_1}{\omega_{c0}}\right)$ because

$$\frac{\left(\frac{a_{i+1}}{\omega_{c0}}\right)^2 - \left(\frac{z_i}{\omega_{c0}}\right)^2}{\left(\left(\frac{z_i}{\omega_{c0}}\right)^2 - x^2\right)\left(\left(\frac{a_{i+1}}{\omega_{c0}}\right)^2 - x^2\right)} > 0, 1 \leqslant i < n-1 \tag{13}$$

as consequence of the verification of the *PZI* property. Then $\Upsilon_x(x,\mathbf{p}) < 0$ in $x \in \left(\frac{a_1}{\omega_{c0}}, \frac{z_1}{\omega_{c0}}\right)$.

Upon differentiating (7), the variation of x with regard to α and $\mathbf{p}$ is obtained:

$$dx = -\frac{x\ln(x)\Upsilon(x,\mathbf{p})}{\alpha\Upsilon(x,\mathbf{p}) + x\Upsilon_x(x,\mathbf{p})} d\alpha - \sum_{k=1}^{2n} \frac{x\Upsilon_k(x,\mathbf{p})}{\alpha\Upsilon(x,\mathbf{p}) + x\Upsilon_x(x,\mathbf{p})} dp_k \tag{14}$$

where $2n$ is the dimension of $\mathbf{p}$ and $\Upsilon_k = \partial\Upsilon/\partial p_k$. The denominator of this expression verifies, substituting (12) there, that

$$\alpha\Upsilon(x,\mathbf{p}) + x\Upsilon_x(x,\mathbf{p}) = \Upsilon(x,\mathbf{p}) \cdot \left(\alpha - \frac{2x^2}{x^2 - \left(\frac{a_1}{\omega_{c0}}\right)^2} - \sum_{i=1}^{n-1} \frac{2x^2\left(\left(\frac{a_{i+1}}{\omega_{c0}}\right)^2 - \left(\frac{z_i}{\omega_{c0}}\right)^2\right)}{\left(\left(\frac{z_i}{\omega_{c0}}\right)^2 - x^2\right)\left(\left(\frac{a_{i+1}}{\omega_{c0}}\right)^2 - x^2\right)} \right) < 0 \tag{15}$$

in $x \in \left(\frac{a_1}{\omega_{c0}}, \frac{z_1}{\omega_{c0}}\right)$ because in that interval: $\Upsilon(x,\mathbf{p}) > 0$, (13) is verified and, since $0 < \alpha \leqslant 1$,

$$\alpha - \frac{2x^2}{x^2 - \left(\frac{a_1}{\omega_{c0}}\right)^2} = -\frac{(2-\alpha)x^2 + \alpha\left(\frac{a_1}{\omega_{c0}}\right)^2}{x^2 - \left(\frac{a_1}{\omega_{c0}}\right)^2} < 0 \tag{16}$$

Next, terms $\Upsilon_k(x,\mathbf{p})$ are calculated in $x \in \left(\frac{a_1}{\omega_{c0}}, \frac{z_1}{\omega_{c0}}\right)$:

1. Gain b, $(k=1)$:

$$\Upsilon_1(x,\mathbf{p}) = \frac{\Upsilon(x,\mathbf{p})}{b} > 0 \tag{17}$$

2. Coefficients $a_i, 1 \leqslant i \leqslant n$, $(k = i+1)$:

$$\Upsilon_k(x,\mathbf{p}) = \frac{2a_i}{\omega_{c0}^2}\left(x^2 - \left(\frac{a_i}{\omega_{c0}}\right)^2\right)^{-1}\Upsilon(x,\mathbf{p}) \tag{18}$$

which verify that $\Upsilon_2(x,\mathbf{p}) > 0$ and $\Upsilon_k(x,\mathbf{p}) < 0$ if $3 \leqslant k \leqslant n+1$.

3. Coefficients $z_i, 1 \leqslant i \leqslant n-1$, $(k = i+1+n)$:

$$\Upsilon_k(x,\mathbf{p}) = \frac{2z_i}{\omega_{c0}^2}\left(\left(\frac{z_i}{\omega_{c0}}\right)^2 - x^2\right)^{-1}\Upsilon(x,\mathbf{p}) > 0 \tag{19}$$

Note that $-x/(\alpha\Upsilon(x,\mathbf{p}) + x\Upsilon_x(x,\mathbf{p})) > 0$ because of inequality (15). Then the sign of $\partial x/\partial p_k$ coincides with the sign of $\Upsilon_k(x,\mathbf{p})$ in expression (14), which justifies Assertion 1 of the theorem, and the sign of term $\partial x/\partial\alpha$ coincides with the sign of $\ln(x)$, which implies that for a given set of parameters $\mathbf{p}$:

- In the case that $x > 1$, increasing α (i.e., increasing ϕ_0, in accordance with (6)) increases the value of x. This means that x is moved away (reaching larger values) from 1 as ϕ_0 increases.
- In the case that $x = 1$, increasing α does not produce any change in x, which is obvious as x^α in (7) is 1 for any value of α.
- In the case that $x < 1$, increasing α (i.e., increasing ϕ_0, in accordance with (6)) decreases the value of x. This means that x is again moved away (reaching smaller values) from 1 as ϕ_0 increases.

Consequently, if ω_c changes as consequence of parameter variations, its deviation from ω_{c0} is amplified if large values of ϕ_0 are used in the controller design. Then Assertion 2 of the theorem has been proven. □

Theorem 4. Consider a plant $G(s,\mathbf{p})$ of the form (1), (2) where $P(s,\mathbf{p})$ verifies the *PZI* property, and $\mathbf{p} \in \mathscr{P}$ such that $\mathbf{p} > 0$ and $\mathscr{P}$ represents the set of all possible plants. Assume a controller $C(s)$ given by expressions (5) and (9) of Theorem 2. The sensitivity of the gain crossover frequency ω_c to changes in the plant parameters has the following properties:

1. Function $f(\mathbf{p})$ is an increasing function in the parameters $p_k, 2 \leqslant k \leqslant n+1$, (a_i) and is a decreasing function in the parameters $p_k, k = 1$, (b), and $n+2 \leqslant k \leqslant 2n$, (z_i).
2. The sensitivity of the gain crossover frequency ω_c, i.e., the variation of ω_c around ω_{c0} when parameters $\mathbf{p}$ vary, increases if the design value ϕ_0 (the opposite of the desired phase margin) increases.

Proof. According to Theorem 2, ω_c belongs to the interval $0 < \omega_c < a_1$, i.e, its normalized value x belongs to $\left(0, \frac{a_1}{\omega_{c0}}\right)$. Since function

$$\Upsilon(x,\mathbf{p}) = \frac{\frac{b}{\omega_{c0}^2}}{\left(\frac{a_1}{\omega_{c0}}\right)^2 - x^2}\prod_{i=1}^{n-1}\left(\frac{\left(\frac{z_i}{\omega_{c0}}\right)^2 - x^2}{\left(\frac{a_{i+1}}{\omega_{c0}}\right)^2 - x^2}\right) \tag{20}$$

is positive in that interval, taking logarithms in this expression, after differentiating with respect to x and following a procedure similar to the one of Theorem 3, the theorem is proven. □

Damped systems

This section studies the damped system

$$G(s,\mathbf{p},\mathbf{q}) = \widehat{G}(s)P(s,\mathbf{p},\mathbf{q}) \tag{21}$$

where

$$P(s,\mathbf{p},\mathbf{q}) = \sum_{i=1}^{n}\frac{k_i}{s^2 + 2a_i\zeta_i s + a_i^2} \tag{22}$$

is a generalization of the partial fraction expansion (4) and $\widehat{G}(s)$ is a rational transfer function that contains the known part of the plant, which is assumed to be stable and minimum phase. All the parameters of (22) are grouped in two uncertainty vectors: $\mathbf{p} = (a_1, a_2, \ldots, a_n, k_1, k_2, \ldots, k_n) \in \mathscr{P}$ being $\mathscr{P}$ the region of admissible parametric vectors, whose elements are positive, and $\mathbf{q} = (\zeta_1, \zeta_2, \ldots, \zeta_n) \in \mathscr{Q}$, being $\mathscr{Q}$ the region of admissible parametric vectors, whose elements are non negative. The first condition is represented by $\mathbf{p} > 0$ and the second one by $\mathbf{q} \geqslant 0$. Coefficients ζ_i of $\mathbf{q}$ have been sorted according to their corresponding a_i. The nominal plant $G(s,\mathbf{p}_0,\mathbf{q}_0)$ is defined by using the nominal parameters $a_{i,0}$, $\zeta_{i,0}$ and $k_{i,0}$. Lemma 1 states that condition $\mathbf{p} > 0$ guarantees that the *PZI* property is verified in $P(s,\mathbf{p},\mathbf{0})$.

Robust phase margin

The following result guarantees a minimum phase margin in the case of damped systems if controllers with the structure (5) and (9) were used.

Theorem 5. Consider system (21), (22) in which $\mathbf{p} \in \mathscr{P}, \mathbf{q} \in \mathscr{Q}$ verify that $\mathbf{p} > 0, \mathbf{q} \geqslant 0$, where $(\mathscr{P},\mathscr{Q})$ is the set of all possible plants. A controller has to be designed that achieves a desired nominal gain crossover frequency ω_{c0} (for $\mathbf{p}_0$, $\mathbf{q}_0$) and:

1. In the case that $a_{1,0} < \omega_{c0} < z_{1,0}$, preserves a phase margin $\phi \geqslant \phi_0$ in all the range of variation of $\mathbf{p}$ and $\mathbf{q}$, where ϕ_0 is a design value $(0 < \phi_0 \leqslant \pi/2$ rads).
2. In the case that $0 < \omega_{c0} < a_{1,0}$, preserves a phase margin $-\phi \leqslant -\phi_0$ in all the range of variation of $\mathbf{p}$ and $\mathbf{q}$, where ϕ_0 is a design value $(0 < \phi_0 \leqslant \pi/2$ rads).

The simplest controller that verifies these conditions is of the form

$$C(s) = K_c s^\alpha \widehat{G}^{-1}(s) \tag{23}$$

where α is given by (6) in the first case and by (9) in the second case. The gain of this controller is given by

$$K_c = \frac{1}{\omega_{c0}^\alpha |P(j\omega_{c0},\mathbf{p}_0,\mathbf{q}_0)|} \tag{24}$$

Proof. Upon operating one of the terms of the partial fraction expansion (22), its imaginary component is obtained:

$$\Im\left\{\frac{k_i}{(j\omega)^2 + j2\cdot a_i\cdot\zeta_i\cdot\omega + a_i^2}\right\} = \frac{-2k_i a_i\zeta_i\omega}{\left(a_i^2 - \omega^2\right)^2 + 4a_i^2\zeta_i^2\omega^2} \leqslant 0 \tag{25}$$

Since this inequality is verified by all the terms of (22) because $\mathbf{p} > 0$ and $\mathbf{q} \geqslant 0$, the imaginary component of $P(j\omega,\mathbf{p},\mathbf{q})$ must be negative or zero.

The frequency response of the open-loop transfer function of system (21), (22) with controller (23) is $L(j\omega,\mathbf{p},\mathbf{q}) = P(j\omega,\mathbf{p},\mathbf{q})K_c\omega^\alpha e^{j\frac{\pi}{2}\alpha}$. Since the imaginary component of $P(j\omega,\mathbf{p},\mathbf{q})$ is negative or zero, its phase would be non positive and would be included in the interval $(-180^\circ, 0^\circ)$. Then the phase of $L(j\omega,\mathbf{p},\mathbf{q})$ would be included in $(-180^\circ + (90\alpha)^\circ, (90\alpha)^\circ)$ because the effect of s^α in the phase of L is a counterclockwise rotation of $(90\alpha)^\circ$ of the frequency response of P. The specifications of the cases 1 and 2 are thus verified if α takes the values stated in the theorem.

Upon imposing the condition of a desired gain crossover frequency to the nominal open-loop transfer function, $|L(j\omega_{c0}, \mathbf{p}_0, \mathbf{q}_0)| = 1$, gain (24) of controller (23) is obtained. □.

Figs. 4 show how the Nyquist plots of Figs. 3a and b are respectively modified as consequence of the controllers proposed in Theorem 5 when damped systems are considered.

Gain crossover frequency sensitivity

Let the plant (22) be expressed in the factorized form

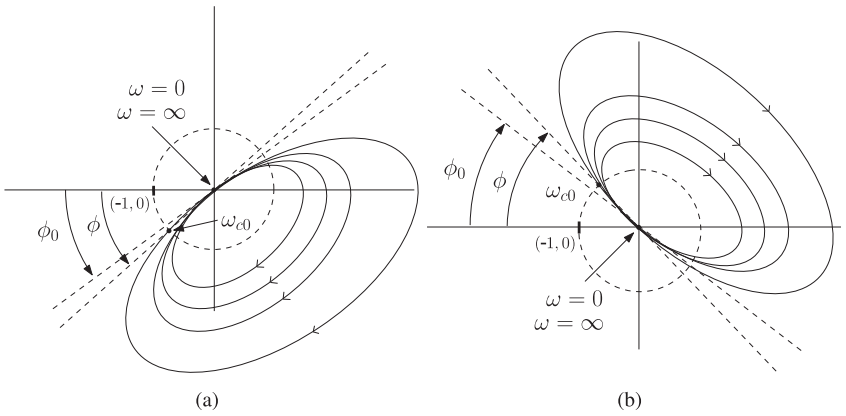

Fig. 4. Nyquist diagrams of the open-loop responses of a damped plant with the controllers of Theorem 5: (a) in Case 1 and (b) in Case 2.

$$P(s,\mathbf{p},\mathbf{q}) = b\frac{\prod_{i=1}^{n-1}(s^2+2z_i\xi_i s+z_i^2)}{\prod_{i=1}^{n}(s^2+2a_i\zeta_i s+a_i^2)} \tag{26}$$

in which any parameter b, z_i and ξ_i depends on all the parameters k_i, a_i and $\zeta_i, 1 \leqslant i \leqslant n$, of (22). In this case function Υ becomes

$$\Upsilon(x,\mathbf{p},\mathbf{q}) = \frac{b}{\omega_{c0}^2}\frac{\prod_{i=1}^{n-1}\left|\left(\frac{z_i}{\omega_{c0}}\right)^2 - x^2 + j2\xi_i\left(\frac{z_i}{\omega_{c0}}\right)x\right|}{\prod_{i=1}^{n}\left|\left(\frac{a_i}{\omega_{c0}}\right)^2 - x^2 + j2\zeta_i\left(\frac{a_i}{\omega_{c0}}\right)x\right|} \tag{27}$$

where $x = \omega/\omega_{c0}$.

Next a theorem that relates the gain crossover frequencies of the system with and without damping is proposed.

Theorem 6. Consider a system (22) in which the magnitude of its frequency response is given by (27). Consider also a controller $C(s)$ of the form (23), (24). Assume that x_c^* is the normalized gain crossover frequency of the system $G(s,\mathbf{p},\mathbf{0})C(s)$ (undamped system) and x_c is the normalized gain crossover frequency of the system $G(s,\mathbf{p},\mathbf{q})C(s)$ (damped system). Moreover, assume that the factors of (27) have bounded damping coefficients:

$$0 \leqslant \zeta_i, \xi_l \leqslant \overline{e} \leqslant \frac{1}{\sqrt{2}}, 1 \leqslant i \leqslant n, 1 \leqslant l \leqslant n-1 \tag{28}$$

and that

$$z_i \approx z_i^*, 1 \leqslant i \leqslant n \tag{29}$$

where z_i^* are the values z_i corresponding to $\mathbf{q} = \mathbf{0}$.

Then an approximate bound for the relative deviation between x_c and x_c^* is:

$$\left|\frac{x_c - x_c^*}{x_c^*}\right| \leqslant \Delta(x_c^*,\mathbf{p},\alpha) = \frac{2\overline{e}^2 max[\lambda_-,\lambda_+]}{|\lambda_0|} \tag{30}$$

where

$$\lambda_0 = \alpha + 2x_c^{*2}\left(\sum_{i=1}^{n}\frac{1}{\left(\frac{a_i}{\omega_{c0}}\right)^2 - x_c^{*2}} - \sum_{i=1}^{n-1}\frac{1}{\left(\frac{z_i}{\omega_{c0}}\right)^2 - x_c^{*2}}\right) \tag{31}$$

$$\lambda_- = \sum_{i=1}^{n-1}\frac{\left(\frac{z_i}{\omega_{c0}}\right)^2}{\left(\left(\frac{z_i}{\omega_{c0}}\right)^2 - x_c^{*2}\right)^2}, \lambda_+ = \sum_{i=1}^{n}\frac{\left(\frac{a_i}{\omega_{c0}}\right)^2}{\left(\left(\frac{a_i}{\omega_{c0}}\right)^2 - x_c^{*2}\right)^2} \tag{32}$$

Proof. Eq. (7) is expressed in the undamped case, with the controller obtained from Theorem 5, as

$$(x_c^*)^{\alpha}\Upsilon(x_c^*,\mathbf{p},\mathbf{0}) = \Upsilon(1,\mathbf{p}_0,\mathbf{q}_0) \tag{33}$$

and can be extended to the damped case as

$$(x_c)^{\alpha}\Upsilon(x_c,\mathbf{p},\mathbf{q}) = \Upsilon(1,\mathbf{p}_0,\mathbf{q}_0) \tag{34}$$

Taking logarithms in these two expressions and substracting them yields

$$\begin{aligned}\alpha\ln(x_c^*) + \ln\left(\Upsilon(x_c^*,\mathbf{p},\mathbf{0})\right) &= \alpha\ln(x_c) + \ln\left(\Upsilon(x_c,\mathbf{p},\mathbf{q})\right)\\ &= \alpha\ln(x_c) + \ln\left(\tfrac{b}{\omega_{c0}^2}\right) +\\ \tfrac{1}{2}\sum_{i=1}^{n-1}\ln\left(\left(\left(\tfrac{z_i}{\omega_{c0}}\right)^2 - x_c^2\right)^2 + 4\xi_i^2\left(\tfrac{z_i}{\omega_{c0}}\right)^2\right) -\\ \tfrac{1}{2}\sum_{i=1}^{n}\ln\left(\left(\left(\tfrac{a_i}{\omega_{c0}}\right)^2 - x_c^2\right)^2 + 4\zeta_i^2\left(\tfrac{a_i}{\omega_{c0}}\right)^2\right)\end{aligned} \tag{35}$$

Approximate (35) by the first term of its expansion into a Taylor series about the values without damping, given by x_c^* and $\mathbf{q} = \mathbf{q}_0 = \mathbf{0}$, and substitute z_i^* by z_i according to (29):

$$\begin{aligned}0 = \tfrac{\alpha}{x_c^*}(x_c - x_c^*) - 2x_c^*\left(\sum_{i=1}^{n-1}\frac{1}{\left(\frac{z_i}{\omega_{c0}}\right)^2 - x_c^{*2}} - \sum_{i=1}^{n}\frac{1}{\left(\frac{a_i}{\omega_{c0}}\right)^2 - x_c^{*2}}\right)(x_c - x_c^*) +\\ 2\sum_{i=1}^{n-1}\frac{\left(\frac{z_i}{\omega_{c0}}\right)^2}{\left(\left(\frac{z_i}{\omega_{c0}}\right)^2 - x_c^{*2}\right)^2}\xi_i^2 - 2\sum_{i=1}^{n}\frac{\left(\frac{a_i}{\omega_{c0}}\right)^2}{\left(\left(\frac{a_i}{\omega_{c0}}\right)^2 - x_c^{*2}\right)^2}\zeta_i^2\end{aligned} \tag{36}$$

Substituting (31) in this expression and rearranging terms gives that

$$\frac{\lambda_0}{2x_c^*}(x_c - x_c^*) = \sum_{i=1}^{n}\frac{\left(\frac{a_i}{\omega_{c0}}\right)^2}{\left(\left(\frac{a_i}{\omega_{c0}}\right)^2 - x_c^{*2}\right)^2}\zeta_i^2 - \sum_{i=1}^{n-1}\frac{\left(\frac{z_i}{\omega_{c0}}\right)^2}{\left(\left(\frac{z_i}{\omega_{c0}}\right)^2 - x_c^{*2}\right)^2}\xi_i^2 \tag{37}$$

Taking into account (28), and that all the summands of the summations of the right hand side of (37) are non negative, inequality (30) is obtained. □

Note that the upper bound of this theorem also applies for the relative deviation of ω_c from ω_c^*, were we denote from now on the gain crossover frequency of the undamped system $G(s,\mathbf{p},\mathbf{0})C(s)$ by ω_c^*.

Theorem 6 allows the application of previous Theorems 3 and 4 - that were developed for undamped systems - to damped systems provided that the bound of (30) is small enough.

Consequently, the following controller design procedure can be summarized:

1. Based on the desired damping, or relative stability, choose the phase margin specification.
2. Choose the fractional order of the controller according to (6) or (9).
3. Tune the gain of the controller in accordance with (24).
   According to Theorem 5, the designed controller guarantees that the phase margin is equal or bigger than the value chosen in step 1) for any set of parameters $\mathbf{p} > 0$ *and* $\mathbf{q} \geqslant 0 \Rightarrow$ *phase margin robustness has been achieved.*
4. Obtain the range of variation of the gain crossover frequency with the parametric variation in the case of the undamped system: $\mathbf{p} > 0$ and $\mathbf{q} = 0$.
5. Determine the modification of the previous range caused by adding damping $\mathbf{q} \geqslant 0$. This modification is determined by the bound $\Delta(x_c^*, \mathbf{p}, \alpha)$ that is calculated using Theorem 6.
6. Check if the obtained range of variation of the gain crossover frequency with the parametric variation $\mathbf{p} > 0$ and $\mathbf{q} \geqslant 0$ is adequate:
   - If yes $\Rightarrow$ the gain crossover frequency robustness has also been achieved and the design procedure ends.
   - If not $\Rightarrow$ go back to step 1) and slightly diminish the phase margin.

The phase margin specification is being diminished until the gain crossover frequency achieves the desired robustness. In this process, if the phase margin goes below a minimum allowed value, the procedure stops because desired simultaneous robustness of the phase margin and gain crossover frequency cannot be achieved.

Control of a single-link flexible robot

This section develops an application in which the previous results are used to damp the vibrations that appear during the fast movement of a very lightweight and slender robot as consequence of its flexibility.

Dynamic model

The robot consists of a DC motor, a slender arm that is attached to the motor hub and two masses floating on an air table. One mass is attached to the middle of the arm and the other to its tip. Fig. 5 shows the arrangement of this two-mass beam. The arm is a piece of music wire (12*in*. long and 0.047*in*. in diameter) clamped to the motor hub. Both masses are fiberglass disks whose centers are attached to the middle and end of the arm with freely pivoted pin joints. The middle disk has a mass m_1 of 0.12*lb*. and the tip mass m_2 can be changed using a set of disks whose masses range from 0.01*lb*. to 0.23*lb*. These disks float on the air table with small friction. Since the mass of the arm is small in comparison to that of these disks and the pinned joints prevent generation of torques in the middle and at the end of the link, this mechanical system behaves practically like an ideal, two-lumped mass flexible arm. A nominal tip mass value $m_{20} = 0.12lb$. is considered.

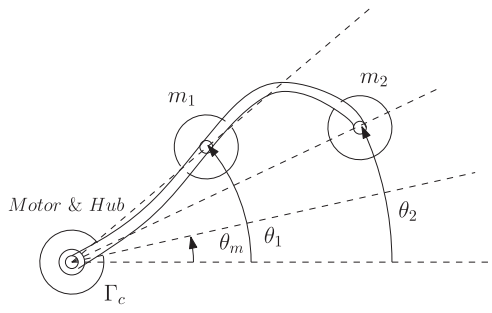

Fig. 5. Scheme of the single-link flexible robot.

In Fig. 5, θ_m represents the motor angle, θ_1 the angle of the middle mass and θ_2 the angle of the tip mass. The measured variables are θ_m and the moment Γ_c at the base of the arm. A dynamic model of this arm was proposed in [21] for the case in which there is no friction at the disks neither internal damping at the link. It is expressed by the following transfer functions, given in function of the tip mass m_2:

$$\frac{\theta_1(s)}{\theta_m(s)} = G_1(s) = \frac{545.7\left(s^2 + \frac{12.733}{m_2}\right)}{s^4 + \left(1455.2 + \frac{21.83}{m_2}\right)s^2 + \frac{6948.4}{m_2}} \tag{38}$$

$$\frac{\theta_2(s)}{\theta_m(s)} = G_2(s) = \frac{-\frac{5.457}{m_2}\left(s^2 - 1273.3\right)}{s^4 + \left(1455.2 + \frac{21.83}{m_2}\right)s^2 + \frac{6948.4}{m_2}} \tag{39}$$

$$\frac{\Gamma_c(s)}{\theta_m(s)} = G_c(s) = \frac{4.11s^2\left(s^2 + 636.65 + \frac{19.1}{m_2}\right)}{s^4 + \left(1455.2 + \frac{21.83}{m_2}\right)s^2 + \frac{6948.4}{m_2}} \tag{40}$$

This model shows two oscillation frequencies ω_{n1} and ω_{n2}, that depend on the value of the carried load m_2, and are obtained from the denominator of these transfer functions.

A high gain loop can be closed around the motor in order to remove the effects of the nonlinear Coulomb and the time varying dynamic frictions, and obtain a very fast response. In order to achieve this, a *PID* feedback control of the motor position θ_m can be implemented that includes compensation terms of the Coulomb friction and the motor-link coupling torque, which is the measured variable Γ_c (see details in [21]). This yields an approximate closed-loop transfer function of the form

$$\frac{\theta_m(s)}{\theta_m^*(s)} = G_m(s) = \frac{1}{(1 + 0.0071s)^2} \tag{41}$$

where $\theta_m^*(t)$ is the reference for the closed-loop motor position control system. $G_m(s)$ is a second order critically damped system with its two poles in -140. Since the coupling torque is compensated in this motor control scheme, $G_m(s)$ is independent of the value of m_2.

Moment Γ_c is feedback for vibration control. Then a transfer function $G(s, \mathbf{p})$ that relates $\theta_m^*(s)$ to $\Gamma_c(s)$ is defined by the product of transfer functions (40) and (41). $G(s, \mathbf{p})$ can be decomposed according to (1) into

$$P(s, \mathbf{p}) = \frac{4.11\left(s^2 + 636.65 + \frac{19.1}{m_2}\right)}{s^4 + \left(1455.2 + \frac{21.83}{m_2}\right)s^2 + \frac{6948.4}{m_2}} = \frac{b\left(s^2 + z_1^2\right)}{\left(s^2 + a_1^2\right)\left(s^2 + a_2^2\right)} \tag{42}$$

and

$$\widehat{G}(s) = \frac{s^2}{(1 + 0.0071s)^2} \tag{43}$$

Parameters in (42) vary as consequence of tip mass changes, being their ranges: $z_1 \in [26.83, 50.46], a_1 = \omega_{n1} \in [4.44, 14.22], a_2 = \omega_{n2} \in [39.12, 58.62]$ and b is the constant value 4.11. Note that the highest value of ω_{n1} is more than three times higher than its lowest value, denoting a significantly large variation of the first vibration mode. Substituting the nominal mass m_{20} in expression (42), the nominal

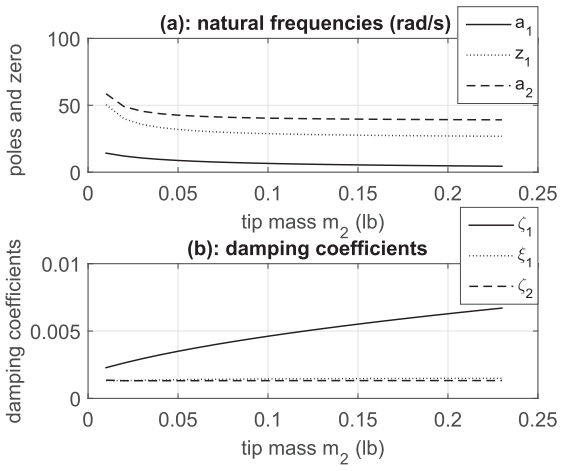

Fig. 6. *PZI* property of transfer function (42).

values of $z_{10} = 28.21 rad/s$, $a_{10} = 6.014 rad/s, a_{20} = 40.011 rad/s$ and $b_0 = 4.11$ are obtained. Fig. 6a plots the evolution of parameters a_1, z_1 and a_2 in function of m_2, illustrating that the *PZI* property is verified in (42).

This dynamics is completed with a damping model of Rayleigh type:

$$\zeta(\omega_n) = \frac{1}{2}\left(\frac{0.059}{\omega_n} + 2.9 \cdot 10^{-5} \cdot \omega_n\right) \tag{44}$$

whose parameters have been tuned from experimental data. If the partial fraction expansion of (42) is carried out:

$$P(s, \mathbf{p}) = \frac{k_1}{s^2 + \omega_{n1}^2} + \frac{k_2}{s^2 + \omega_{n2}^2} \tag{45}$$

this expression is modified to

$$P(s, \mathbf{p}, \mathbf{q}) = \frac{k_1}{s^2 + 2\zeta_1 \omega_{n1} s + \omega_{n1}^2} + \frac{k_2}{s^2 + 2\zeta_2 \omega_{n2} s + \omega_{n2}^2} = \frac{b\left(s^2 + 2\xi_1 z_1 s + z_1^2\right)}{\left(s^2 + 2\zeta_1 a_1 s + a_1^2\right)\left(s^2 + 2\zeta_2 a_2 s + a_2^2\right)} \tag{46}$$

where the damping coefficients ζ_i are obtained from (44) substituting the vibration frequencies ω_{ni}. Fig. 6b shows the variation of ζ_1, ξ_1 and ζ_2 in function of m_2.

Control system

Strain (moment) feedback has already been used to achieve robust control of single link flexible robots whose parameters undergo large changes. Feedback of a linear combination of the torque at the base of the arm and its integral was reported in [22]. A nonlinear controller based on the feedback of these two signals was reported in [23] and a linear controller that also uses these two signals was proposed in [24] which was based on a passivity property of the arm. Strain feedback laws proposed in [22,24] basically implement *PI* controllers that guarantee stability robustness to large parametric changes. The controller developed here guarantees not only stability - as the other control design methods do - but also a desired minimum phase margin (or damping) when large parametric variations are produced.

In this paper, the combined feedforward-feedback control system shown in Fig. 7 is proposed. The feedforward term $F(s)$ and the feedback term $C(s)$ of this figure have to be designed.

Closed-loop controller design: $C(s)$

A controller with the following specifications is desired:

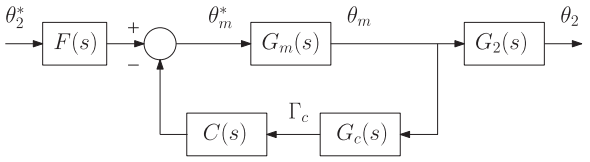

Fig. 7. Control scheme of the flexible robot.

1. A damping coefficient $\hat{\zeta}_0 = 0.7$. The phase margin that yields this damping is obtained from the expression $\phi_0 \approx 100\hat{\zeta}_0 = 70^\circ$, which was originally developed for second-order systems (e.g., [5]).
2. A nominal settling time of $t_{s0} = 0.4s$. Application of the approximate relation $\omega_c \approx 4/t_s$ yields a gain crossover frequency $\omega_{c0} \approx 10 rad/s$.
3. Zero steady state error to a step reference of the tip angle $\theta_2^*(t)$.
4. Robust isophase margin condition: it is desired to maintain a phase margin $\phi \geqslant \phi_0$ of the two vibration modes for any value of m_2 in the range $0.01lb.$ to $0.23lb.$

Since the chosen ω_{c0} verifies that $a_{10} < \omega_{c0} < z_{10}$, the first case of Theorem 5 is applied to obtain the parameters of (23). Then formula (6) yields a value $\alpha \approx 0.8$ and (24) yields a value $K_c \approx 5.31$.

Controller (23) is therefore

$$C(s) = \frac{(1 + 0.0071s)^2}{s^2} 5.31 s^{0.8} \tag{47}$$

Factor $(1 + 0.0071s)^2$ can be approximated by $1 + 0.0142s$ in the range of frequencies of interest $[0, 60]$ rad/s (it is up to the highest vibration frequency, that corresponds to the second vibration mode in the case of $m_2 = 0.01lb.$). Fig. 8 illustrates the closeness of the Bode diagrams of these two factors in that frequency range by plotting $Q(j\omega) = (1 + j0.0142\omega)/(1 + j0.0071\omega)^2$. The maximum deviation from unity of $Q(j\omega)$ in that range is $+0.91$ dB in magnitude and -5.5° in phase, which is considered acceptable. Then controller (47) can be approximated by

$$C(s) = \frac{5.31(1 + 0.0142s)}{s^{1.2}} \tag{48}$$

Denote as ω_{c1} and ω_{c2} the values of the gain crossover frequencies associated to the first and second vibration modes respectively, and ϕ_1 and ϕ_2 their corresponding phase margins. Table 1 shows the values of $\omega_{c1}, \omega_{c2}, \phi_1$ and ϕ_2 of the compensated open-loop transfer functions

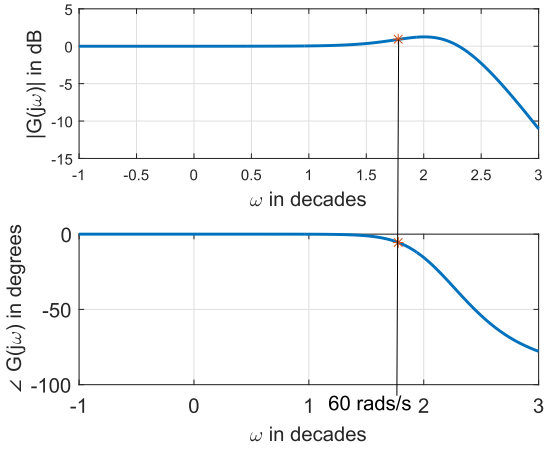

Fig. 8. Bode diagrams of $Q(s) = \frac{1+0.0142s}{(1+0.0071s)^2}$.

Table 1
Frequency specifications with the fractional-order controller.

$m_2(lb)$	ω_{c1} (rad/s)	$\phi_1(^\circ)$	ω_{c2} (rad/s)	$\phi_2(^\circ)$
0.01	19.2	72.2	60.4	68.4
0.12	10	72.5	43.4	70.2
0.23	8.6	72.5	42.6	70.3

$$L(s,\mathbf{p},\mathbf{q}) = G_m(s)G_c(s)C(s) = 5.31s^{0.8}P(s,\mathbf{p},\mathbf{q})G_m(s)(1+0.0142s) \quad (49)$$

in the cases of the lowest, nominal and highest values of the tip mass m_2. This table shows that specification $\omega_{c0} = 10$ rad/s is verified in the case of the nominal payload $m_2 = 0.12$ lb. (it corresponds to the value ω_{c1} of the table). Moreover, specification $\phi_0 = 70^\circ$ is verified by the two gain crossover frequencies ω_{c1} and ω_{c2} in the case of the nominal m_2. The results in the case of the nominal payload that are shown in this table slightly differ from the design specifications. It is caused by the small difference existing between the exact value of the fractional order of the differentiator in (47), which is 0.78, and the rounded value of 0.8 that is being used, and by the approximation carried out of the factor $(1+0.0071s)^2$. Note that the phase margins associated to the two vibration modes in the cases of the two extreme payloads remain always close to 70°, as expected from the fulfillment of Theorem 5.

Feedforward term design: $F(s)$

The closed-loop transfer function of the scheme of Fig. 7 is

$$H(s) = \frac{\theta_2(s)}{\theta_2^*(s)} = \frac{F(s)G_m(s)G_2(s)}{1+C(s)G_m(s)G_c(s)} \quad (50)$$

In order to improve the speed of response of this system, a proper feedforward term is proposed of the form

$$F(s) = \frac{1+f_n s^\beta}{1+f_d s}, \beta \in \Re \quad (51)$$

Specification 3 is verified if $H(0) = 1$. Since $F(0) = G_m(0) = G_2(0) = 1$, the specification is accomplished if $C(0)G_m(0)G_c(0) = 0$, which is true if $\alpha > 0$. Since $\alpha = 0.8$ in our design, the specification is verified.

Parameters β, f_n and f_d are given by an optimization process in which the frequency range at which the magnitude of $H(j\omega)$ is inside a bandwidth of ±0.3 dB around 0 dB is maximized. It is carried out for the nominal plant under the following constraints: $0 \leqslant f_n, 0 < f_d$, and $0 < \beta \leqslant 1$. The resulting optimal prefilter is

$$F(s) = \frac{1+0.116s^{0.55}}{1+0.011s} \quad (52)$$

that yields the overall frequency response shown in Fig. 9. The closed-loop system bandwidth (defined with a threshold of 3 dB on the magnitude of the $H(j\omega)$) of the nominal plant using prefilter (52) is 10 rad/s, which is considered adequate to provide a fast response.

Overall performance

The following command signal θ_2^* is defined in order to carry out simulations of the time performance of the controlled system:

$$\begin{cases} \theta_2^*(t) = 0.5(1-cos(\frac{\pi}{T}t)), 0 \leqslant t \leqslant T \\ \theta_2^*(t) = 1, t > T \end{cases} \quad (53)$$

which is a smoothed unity step command, in order to avoid unbounded velocities and accelerations. A value $T = 0.1$ s is used.

Fig. 10 shows the responses to the command signal (53) of the moment Γ_c at the base of the arm and the tip angle θ_2 in the cases in which the payload m_2 has its nominal and extreme values, when the control system of Fig. 7 is used with controller (48) and prefilter (52).

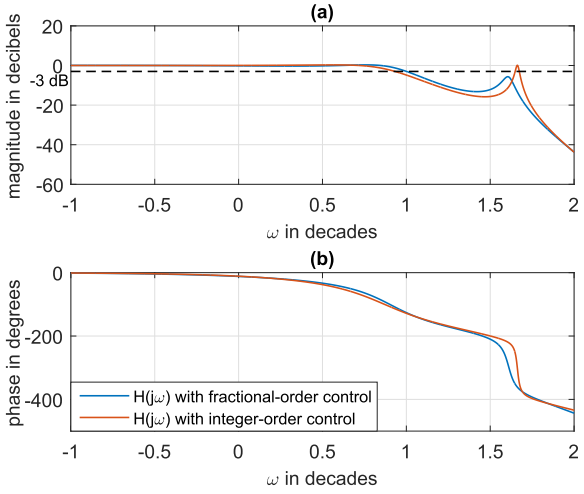

Fig. 9. Frequency responses of the overall closed-loop control of the nominal systems $H(s)$ using fractional and integer order control systems.

Comparison with an integer order controller

For comparison purposes, a *PI* controller has also been designed that verifies the same Specifications 1 to 3 for the nominal plant as before. This design is carried out taking into account the complete dynamics $P(s,\mathbf{p},\mathbf{q})\widehat{G}(s)$, and yields:

$$C(s) = -0.072 + \frac{3.29}{s} \quad (54)$$

Table 2 shows the values of the gain crossover frequencies ω_{c1}, ω_{c2}, associated to each of the two vibration modes and their corresponding phase margins, ϕ_1, ϕ_2, in the cases of the three previously considered tip payloads. Specifications $\omega_{c0} = 10$ rad/s and $\phi_1 = 70^\circ$ are verified in the case of the nominal payload $m_2 = 0.12$ lb. The phase margin ϕ_1 changes noticeably with m_2, but its value is maintained high enough in all the cases. However, ϕ_2 is very low in all the cases, being the second vibration mode unstable when $m_2 = 0.01$ lb. (a negative phase margin is shown).

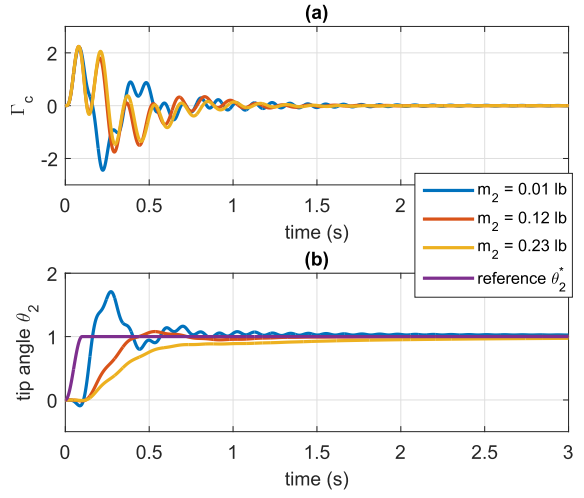

Fig. 10. Responses to the command signal (53) of: (a) the moment Γ_c at the base of the arm and (b) the tip angle θ_2, for different payloads m_2, when the fractional-order control system is used.

Table 2
Frequency specifications with the *PI* controller.

$m_2(lb)$	ω_{c1} (rad/s)	$\phi_1(^\circ)$	$\omega_{c2}(rad/s)$	$\phi_2(^\circ)$
0.01	20.2	50	62.1	−10.5
0.12	10	70	45.9	9.1
0.23	8.4	73.2	45.2	10

Repeating the optimization process carried out to tune the parameters of prefilter (51), but taking into account that the *PI* controller (54) is used now, yields that

$$F(s) = \frac{1 + 0.025s}{1 + 0.017s} \tag{55}$$

It is mentioned that the range of search for β was increased later to $0 < \beta \leqslant 1.2$ in order to check if $\beta = 1$ really yielded the global maximum. In that new search, the optimal order of β was again 1 with the coefficients of (55). Then the integer order filter is the optimal filter in this case. The overall frequency response $H(j\omega)$ of the control system using the *PI* controller (54) and prefilter (55) is shown in Fig. 9 labeled as '$H(j\omega)$ with integer-order control'. Its bandwidth (defined with a threshold of 3 dB) is 8.6 rad/s, which is lower than the one achieved using the fractional-order control.

It is easy to check that controller (54) verifies the condition $C(0)G_m(0)G_c(0) = 0$, needed to obtain that $H(0) = 1$. Then Specification 3 is verified by this control system.

Fig. 11 shows the responses to the command signal (53) of the moment Γ_c at the base of the arm and the tip angle θ_2 in the cases in which the payload m_2 has its nominal and extreme values, when the control system of Fig. 7 is used with the *PI* controller (54) and prefilter (55).

Comparing Figs. 10 and 11, it is observed that:

- The first mode is quickly removed in the cases of the three masses using both fractional and integer order controllers.
- The responses of Fig. 11 are significantly more oscillatory than the responses of Fig. 10. This is more noticeable in the responses of Γ_c: since the moment at the base of the arm is directly related to angular accelerations and accelerations are the second derivative of angular positions, the vibrations of the tip angle can be observed highly amplified in Γ_c. In particular, the second vibration mode, which is the main oscillation observed in these figures, is damped more quickly in Fig. 10 than in Fig. 11 for the three tip masses.
- The *PI* controller is very inefficient in damping the oscillations of the second mode when low payloads have to be carried. In fact, the vibrations are amplified (unstable system) in the case of the lowest value of m_2.

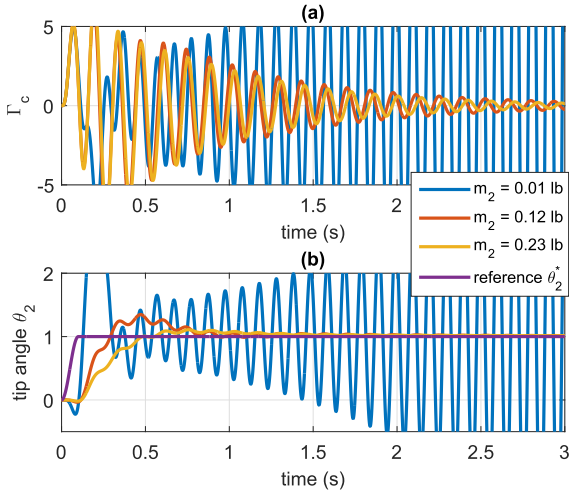

Fig. 11. Responses to the command signal (53) of: (a) the moment Γ_c at the base of the arm and (b) the tip angle θ_2, for different payloads m_2, when the integer-order control system is used.

Comparison with a controller designed with other phase margin

The theorems developed in this paper can also be applied in the integer order case, which corresponds to a design phase margin $\phi_0 = 90^\circ$ that yields a value $\alpha = 1$. This suggests that an integer order controller (5) or (9) could be used instead of a fractional order controller, that would increase the phase margin attained with (48), would maintain the previously mentioned robustness properties and could be much more easily implemented than (48).

Then a controller is designed with the same specifications of (48) except for the phase margin specification, which is now $\phi_0 = 90^\circ$. This controller is

$$C(s) = \frac{3.35(1 + 0.0142s)}{s} \tag{56}$$

The gain crossover frequency robustness of the system with this controller is studied next.

Consider the undamped system. Expression (40) shows that parameters a_1, a_2 and z_1 of (42) diminish as m_2 increases (it can also be observed in Fig. 6a) while b remains constant. Then, according to the first part of Theorem 3, the $f(\mathbf{p})$ function must be decreasing with m_2 and, according to the second part of this theorem, the range of variation of ω_c^* must increase with the value of the phase margin specification.

Functions $\omega_c^* = f(\mathbf{p})$ of the undamped system obtained with controllers (48) and (56) - designed for a $\omega_{c0} = 10$ rad/s and nominal phase margins $\phi_0 = 70^\circ$ and $\phi_0 = 90^\circ$ respectively - were calculated numerically. These functions agree with the results predicted by Theorem 3: decreasing curves are obtained and the range of variation of ω_c^* is higher in the case of the controller designed for $\phi_0 = 90^\circ$ than in the case of the controller designed for $\phi_0 = 70^\circ$. In the case of $\phi_0 = 90^\circ$, this range is $[8.4, 20]$ rad/s and in the case of $\phi_0 = 70^\circ$, is $[8.6, 19.2]$ rad/s. It means that using the integer-order controller increments the range obtained with (48) in 9.4%, and reduces therefore the robustness of ω_c^* in this percentage. The ω_c^* range is $[8.7, 18.5]$ rad/s in the case of the controller designed with a $\phi_0 = 50^\circ$ ($\alpha = 0.56$). The use of the integer order controller (56) reduces in 18.4% the ω_c^* robustness attained by this last controller.

Subsequently, the bound Δ defined in (30) is calculated. Fig. 6b shows that an upper bound of the damping coefficients for all the range of variation of m_2 is $\bar{e} = 0.007$. Moreover, it is easy to prove analytically that $z_1 = z_1^*$ in the case of $n = 2$, and then condition (29) becomes an identity in the case of our robot. Coefficients λ_0, λ_- and λ_+ are calculated for each value of m_2 using (40) and the functions $\omega_c^* = f(\mathbf{p})$ previously obtained (which allow to calculate x_c^* as ω_c^*/ω_{c0}). Function $\Delta(m_2)$ has a maximum of $2.1 \cdot 10^{-5}$ in the case of controller (48) and of $2.2 \cdot 10^{-5}$ in the case of (56). These very low values guarantee that the relative error between ω_c and ω_c^* is very low for all the range of parametric variations and, then, the results obtained for the undamped plant regarding the gain crossover frequency robustness can also be extended to our lightly damped system. Functions $\omega_c = f(\mathbf{p}, \mathbf{q})$ were calculated numerically later just for validation purposes. They are very close to $\omega_c^* = f(\mathbf{p})$. Then the validity of extending the results obtained for the undamped system to our damped system is confirmed.

Conclusions

This article has addressed the problem of robustly damping the vibrations of oscillatory systems with large uncertainties in their parameters. Moreover, general solutions have been searched that allow to confront systems with an arbitrary number of vibration modes. In theory, the proposed controller is able to robustly damp vibrations of systems with an infinite number of vibration modes (just make $n = \infty$ in model (2)). This implies that our control system is robust to spillover effects, i.e., to the unstabilizing effects caused by the vibration modes that are usually neglected in the controller design (this may be especially important in infinite dimensional systems represented by partial differential equations).

Our controller outperforms other robust control systems in the sense that it not only guarantees closed-loop stability but also a desired damping of all the vibration modes, defined by a minimum phase margin specification for all the vibration modes (robust isophase margin control).

It was proven in a previous paper of [20] that the controller used here has the above robustness properties if the transfer function of the system has the so called pole-zero interlacing property on the imaginary axis. This is not an intrinsic property of an oscillatory system. It depends on the input and output (measured) variables that are chosen.

The results shown in Theorems 1 and 2 of [20] were obtained for undamped systems and focused on the phase margin robustness. The contributions of the present paper are: (1) an analysis of the gain crossover frequency robustness of the proposed fractional-order controllers carried out for undamped systems in Theorems 3 and 4, (2) the extension of the previous phase margin robust control results to damped systems in Theorem 5 and (3) the extension of the gain crossover frequency robustness analysis performed in 1) to damped systems in Theorem 6.

A consequence of Theorems 3 and 4 is that values of α closer to unity produce larger variations in the gain crossover frequency when parameters change (which implies larger variations of the speed of the response). Moreover, the controller amplifies the high frequency noise of the system more as α increases. These two considerations advise the use of controllers with fractional orders sensibly lower than unity (further away from the integer-order controller). Then a gain crossover frequency such that $a_{1,0} < \omega_{c0} < z_{1,0}$ is suggested in order to obtain a value of α lower than 1 as well as the use of Theorem 1, since the use of Theorem 2 would yield a controller with a fractional order higher than 1.

It was mentioned in the Introduction that other methods have been developed to design fractional-order controllers that achieve isophase margin robustness. However, these methods provide only a *local* isophase margin property, i.e, the phase plot of the frequency response of the open-loop transfer function is flat only in a small range of frequencies around the design gain crossover frequency. This implies that the phase margin is maintained constant only when small parametric changes are produced. Instead, our method is the only one that achieves a *global* isophase margin property, i.e, the phase plot of the frequency response of the open-loop transfer function is flat in all the frequency range $0 \leqslant \omega < \infty$ with the exception of a finite number of isolated points. This implies that the phase margin is maintained constant even in the case that very large parametric variations are produced.

Theorems 1 and 2 proved that any controller that achieves the *global* isophase margin property in an undamped system (1)–(2) must contain a factor of a fractional-order nature. Moreover, the same result was proven in Theorem 5 for a damped system (21)-(22) (in this case the *global* isophase margin property is redefined as the property of achieving a phase margin bigger than a given value in all the range $0 \leqslant \omega < \infty$, i.e, a damping bigger than a given value).

Then, it is remarked that the above *global* robust specification cannot be obtained using integer order controllers and, hence, well-known robust techniques like the H_∞ method or the μ-framework are precluded. In order to achieve the *global* robust phase margin specification, the whole Nyquist plot of the open-loop frequency response has to be adequately shaped. Our method allows such shaping, unlike the mentioned robust controller design methods, that only attain desired values of some norms of the open-loop frequency response.

QFT techniques are the only ones that allow shaping the Nyquist plot in a large range of frequencies. However, in our robustness problem, in which large variations of parameters and an arbitrary number of resonant modes are considered, the shaping must be carried out in all the frequency range $0 \leqslant \omega < \infty$. Any *QFT* design that attempts to achieve this specification using standard integer-order controllers yields very high order transfer functions that are simply approximations of our proposed fractional-order exact controllers. This was illustrated in [25], where a fractional-order controller similar to the ones developed in this paper was designed in order to achieve the *global* isophase margin property and cope with very large changes of a time constant. The obtained controller was compared to a *QFT* design, which yielded a controller transfer function of very high order that was able to preserve the robust phase margin specification in only a limited interval of values of the time constant. Then, if the *global* isophase margin condition is pursued, the only alternative to our fractional-order controller is using integer order controllers of very high order (which could imply controller fragility and implementation problems).

These results have been applied to the design of a robust controller for the vibration free movement of a robot with a flexible link whose payload is time varying. This variation produces large changes in the frequency of the first vibration mode (the highest value is more than three times higher than the lowest value). The use of most of the developed theorems has been illustrated in this example.

Finally, it should be mentioned that fractional-order controllers can be implemented using a variety of techniques, e.g., [26], and their practical realizations with computers do not imply any particular problem.

Declaration of Competing Interest

The authors certify that they have no affiliations with or involvement in any organization or entity with any financial or non-financial interest in the subject matter or materials discussed in this manuscript.

Compliance with Ethics Requirements

This article does not contain any studies with human or animal subjects.

Acknowledgments

This research was sponsored in part by the Spanish Government Research Program with the project DPI2016-80547-R (Ministerio de Economía y Competitividad), in part by the University of Castilla-La Mancha under Project 2019-GRIN-26969 and in part by the European Social Fund (FEDER, EU).

References

[1] Guo M, Crow M, Sarangapani J. An improved UPFC control for oscillation damping. IEEE Trans Power Syst 2009;24(1):288–96.
[2] Parreño A, Roncero-Sanchez P, Feliu-Batlle V. A two degrees of freedom resonant control scheme for voltage-sag compensation in dynamic voltage restorers. IEEE Trans Power Electron 2018;33(6):4852–67.
[3] Ziada S, Graf H. Feedback control of combustion oscillations. J Fluids Struct 1997;12:491–507.
[4] Ramli L, Mohamed Z, Abdullahi A, Jaafar H, Lazim I. Control strategies for crane systems: a comprehensive review. Mech Syst Signal Process 2017;95:1–23.
[5] Ogata K. Modern control engineering. Prentice hall; 1993.
[6] Zhang K, Scorletti G, Ichchou M, F M. Quantitative robust linear parameter varying H_{infty} vibration control of flexible structures for saving the control energy. J Intell Mater Syst Struct 2015;26(8):1006–27.
[7] Steinbuch M, Groos P, Schootstra G, Wortelboer P, Bosgra O. μ-synthesis for a compact disc player. Int J Robust Nonlinear Control 1998;8:169–89.
[8] Mahmoodi M, Mills J, Benhabib B. A modified integral resonant control scheme for vibration suppression of parallel kinematic mechanisms with flexible links. Int J Mechatron Autom 2015;5(1):44–57.
[9] Dastjerdi A, Vinagre B, Chen Y, HosseinNia H. Linear fractional order controllers; a survey in the frequency domain. Annu Rev Control 2019;47:51–70.
[10] Manabe S. A suggestion of fractional-order controller for flexible spacecraft attitude control. Nonlinear Dyn 2002;29(1–4):251–68.
[11] Oustaloup A, Moreau X, Nouillant M. The crone suspension. Control Eng Pract 1996;4(8):1101–8.
[12] Becedas J, Trapero J, Feliu-Batlle V, Sira-Ramirez H. Adaptive controller for single-link flexible manipulators based on algebraic identification and generalized proportional integral control. IEEE Trans Syst, Man Cybernet Part B 2009;39(3):735–51.
[13] Cui L, Chen W, Wang H, Wang J. Control of flexible manipulator based on reinforcement learning. In: Proceedings of the 2018 Chinese Automation Congress (CAC), Xian (China), IEEE; 2018.
[14] Haung A, Liao K. FAT-based adaptive sliding control for flexible arms: theory and experiments. J Sound Vib 2006;298(1–2):194–205.
[15] Preumont A. Vibration control of active structures: an introduction; 2011.
[16] Badkoubeh A, Zheng J, Zhu G. Flatness-based deformation control of an euler-bernoulli beam with in-domain actuation. IET Control Theory Appl 2016;10(16):2110–8.
[17] Huang D, Zhou S, Li W. Vibration suppression of a viscoelastic isolation system by nonlinear integral resonant controller. J Vib Control 2019;25(10):1599–613.
[18] Feliu-Talegon D, San-Millan A, Feliu-Batlle V. Fractional-order integral resonant control of collocated smart structures. Control Eng Pract 2016;56:210–23.
[19] Feliu-Talegon D, Feliu-Batlle V. Passivity-based control of a single link flexible manipulator using fractional controllers. Nonlinear Dyn 2019;95(3):2415–41. https://doi.org/10.1007/s11071-018-4701-4.
[20] Feliu-Batlle V. Robust isophase margin control of oscillatory systems with large uncertainties in their parameters: a fractional-order control approach. Int J Robust Nonlinear Control 2017;27(12):2145–64.
[21] Feliu-Batlle V, Rattan K, Brown HJ. Modeling and control of single-link flexible arms with lumped masses. ASME J Dynam Syst, Meas Control 1992;114:59–69.
[22] Luo Z. Direct strain feedback control of flexible robot arms: new theoretical and experimental results. IEEE Trans Autom Control 1993;38(11):1610–22.
[23] Ge S, Lee T, Zhu G. Improving regulation of a single-link flexible manipulator with strain feedback. IEEE Trans Robot Autom 1998;14(1):179–85.
[24] Feliu-Batlle V, Pereira E, Diaz I. Passivity-based control of single-link flexible manipulators using a linear strain feedback. Mech Mach Theory 2014;71:191–208.
[25] Feliu-Batlle V, Castillo F. On the robust control of stable minimum phase plants with large uncertainty in a time constant. a fractional-order control approach. Automatica 2014;50(1):218–24.
[26] Vinagre B, Feliu-Batlle V, Tejado I. Fractional control: Fundamentals and user guide. Revista Iberoamericana de Automática e Informática Industrial 2016;13(3):265–80.